Geotechnical conditions and ice loading for an offshore drilling platform in the Canadian Beaufort Sea

Scott Martens, Arash Eshraghian & Brian Rogers
Klohn Crippen Berger Ltd., Calgary, Alberta, Canada

ABSTRACT
The SDC mobile arctic drilling platform was deployed 50 km offshore in a water depth of 14 m at the Paktoa site in the Canadian Beaufort Sea over the winter of 2005-2006. Geotechnical investigations were done from the landfast ice prior to deployment and from the SDC deck. An ice loading event in February 2006 resulted in measurable displacements in the in-place inclinometer string below the SDC. Several analysis methods were used to estimate the magnitude of the ice load during this event, to provide a better understanding of the magnitude of ice loading for future arctic deployments of gravity based drilling platforms.

RÉSUMÉ
Pendant l'hiver 2005-2006, la plateforme de forage arctique de SDC a été déployée sur le site de Paktoa, à 50 km des côtes dans la mer de Beaufort canadienne, dans une région où la profondeur de l'eau atteint 14 mètres. Des examens géotechniques ont été réalisés sur la glace de rive avant le déploiement et sur la plateforme de SDC. Une surcharge de glace survenue en février 2006 a provoqué un déplacement mesurable de l'inclinomètre intégré sous la plateforme de SDC. De nombreuses méthodes d'analyse ont été utilisées pour évaluer l'amplitude de la surcharge lors de l'événement afin de mieux comprendre l'effet d'une surcharge de glace pour les futurs déploiements de plateformes à embase gravitaire dans l'arctique.

1 INTRODUCTION

The Steel Drilling Caisson (SDC) is a bottom founded mobile offshore drilling unit capable of operating in 8 m to 25 m of water in the Beaufort Sea environment. The unit consists of a steel drilling caisson mated to a submersible barge, referred to as the MAT. The SDC deck is 60 m wide and 218 m long, and the MAT base is 110 m by 162 m. The large base area of the MAT, together with 2 m deep steel skirts, enables the SDC to resist large ice forces on the structure at sites with relatively weak soils without the need for site preparation. Details of the SDC and MAT are discussed in Hewitt et al. (1987). To date, the SDC has been deployed at eight sites in the Canadian and Alaskan Beaufort Sea.

This paper addresses geotechnical aspects of the SDC deployment at the Paktoa C-60 site in the Canadian Beaufort Sea, at approximately 69°39'N 136°29'W. The Paktoa location is shown on Figure 1. A photo of the SDC at Paktoa is shown in Figure 2.

2 SITE DESCRIPTION

The Canadian Beaufort Shelf has been subdivided into a number of physiographic regions, based on the physical properties of the surficial sediments. These regions consist of a series of submerged plateaus and troughs, with a trend to more fine grained sediments to the west (O'Connor 1980, 1982, Blasco 1990). In general terms, the plateaus have more coarse gained sediments and high strength silts and clays and thus provide better foundation conditions. In the trough regions, greater depths of soft silts and clays are present, particularly in the Mackenzie trough to the west.

The Paktoa site is located near the edge of the Mackenzie Trough physiographic region. The water depth across the SDC setdown footprint (corrected for tidal variation) varies between 12.75 m and 14.25 m, due to ice scouring on the seabed. The surficial sediments within this depression consist of soft to firm silts and clays with occasional interbedded sand layers, which have probably been deposited within the last 25,000 years and are geologically young. Permafrost is not present in the seabed soils at the Paktoa site.

Figure 1. Paktoa site location

2.1 Site Investigations

Klohn Crippen Berger performed the first stage of the geotechnical investigation at the Paktoa site from the landfast ice in April 2005. During that investigation, Cone Penetration Tests (CPT) were performed at three locations, with associated insitu vane shear tests and tube sampling of the seabed soils. The CPT holes in the April 2005 investigation were pushed by a lightweight drill rig with casing from the ice surface to the mudline, and test depths ranged from 10.5 m to 12 m below mudline. The casing was required to support the CPT rods through the water, to prevent buckling of the CPT rods. The drill rig was bolted to the ice to provide reaction force for pushing the CPT. A low-capacity CPT cone was used to achieve good strength resolution in the soft upper soils. The drill rig used was a MARL M2.5T track-mounted heliportable auger drill. The CPT and drill setup are shown on Figure 3.

Figure 2. SDC at Paktoa C-60 site

Two Shelby tube and two piston tube samples were obtained from depths in the range of 1.0 m to 3.6 m below seabed. Five in-situ vane shear tests were done in the upper 2.5 m. The lab testing program included Atterberg limits, one-dimensional consolidation and consolidated-undrained triaxial tests.

Additional investigations were performed from the deck of the SDC following the SDC setdown at the Paktoa site in September 2005. The program from the deck of the SDC allowed for a greater depth of the seabed to be investigated compared to the April 2005 program, and for instrumentation to be installed in the seabed to monitor foundation pore pressures and displacements during and following any significant ice loading events.

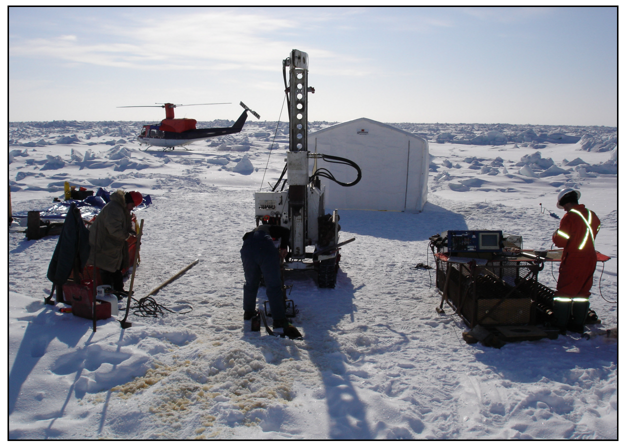

Figure 3. CPT setup from ice at Paktoa 50 km offshore

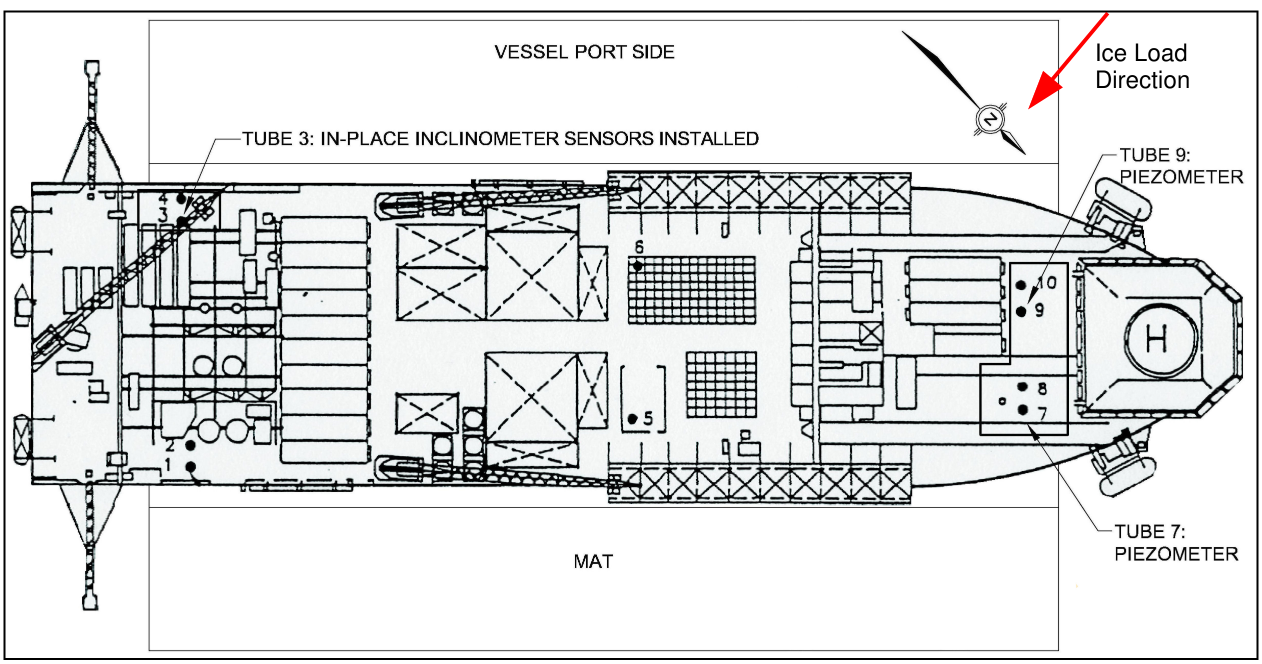

Figure 4. SDC plan and instrument locations

The geotechnical investigation from the deck of the SDC was performed through tubes that extend from the deck surface to the base of the SDC. The tubes are approximately 250 mm inside diameter steel pipes within the SDC, and connect to 1 m diameter circular openings through the MAT. Heavy steel casings were installed to support the CPT rods and prevent buckling of the rods during pushing from the SDC deck due to the 40 m unsupported distance between the deck and the seabed.

A total of three CPT soundings were performed in September 2005 at Tubes #4, #7, and #9 (denoted CPT05-T4, CPT05-T7 and CPT05-T9). Tube #3 was drilled for sampling, vane shear testing and installation of an inclinometer casing (denoted BH05-T3). A total of 8 insitu shear vane tests were performed in the upper 12 m and 5 samples were taken using a hydraulic piston sampler. The investigation and instrument locations are shown on the plan of the SDC on Figure 4.

In both investigations, the drilling, CPT and sampling were performed by ConeTec Investigations Ltd. of Vancouver, B.C.

2.2 Soil Description and Properties

The subsurface soils were characterized as medium to high plastic, silty clay. The clay was very soft near the seabed but rapidly increased in strength up to 2 m depth. The clay was dark grey, with occasional thin, very dark grey organic layers. Individual shells were occasionally found within the soil matrix. The clays recovered in the sample tubes were typically massive, with little to no bedding visible.

Liquid limits ranged from 43% to 58%, with a trend of increasing liquid limit with depth, and natural water contents from 35% to 54%. The liquidity indices were typically in the range of 0.4 to 0.9, indicating that the soils were normally to lightly overconsolidated.

The dynamic pore pressure response measured with the CPT was negative in the upper few metres, also indicating that the clays are overconsolidated. Below approximately 3 m, the pore pressure response was strongly positive, indicating that the clay is normally consolidated or lightly overconsolidated.

The undrained shear strength of the seabed soils was estimated from the CPT data using Equation [1]:

$$S_u = \frac{q_t - \sigma_v}{N_{kt}} \qquad [1]$$

where:

S_u = undrained shear strength (interpreted)

q_t = tip stress corrected for unequal end area

σ_v = vertical total stress

N_{kt} = empirical factor relating CPT resistance to undrained shear strength

Previous investigators have recommended that the undrained shear strength calculated from the CPT use N_{kt} values in the range of 10 to 14 (Jefferies et al, 1985) or 15 (Weaver and Poplin, 1997). A N_{kt} value of 14 was used to calculate the undrained shear strength from the CPT tip resistance at Paktoa, based on correlations between the CPT data and the vane shear tests. The undrained shear strength from the insitu vane shear tests and the strength calculated from the CPT using this N_{kt} factor are plotted together on Figure 5. An undrained strength ratio Su/p'=0.25 typical of Beaufort Sea clays based on the work of Shinde et al. (1986) is also plotted on Figure 5. A comparison of this line with the undrained strengths interpreted from the CPT indicates that the clays are more heavily overconsolidated near the seabed, with the overconsolidation ratio decreasing with depth.

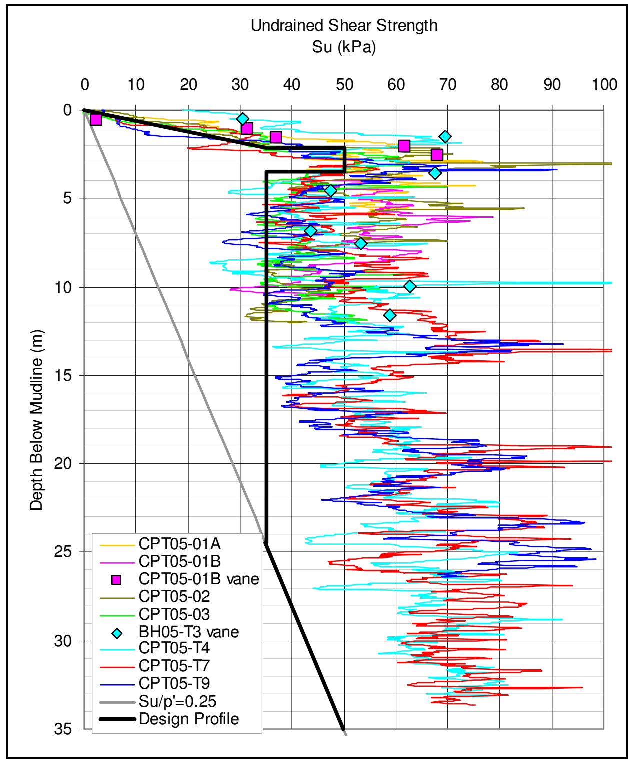

Figure 5. Undrained shear strength profile

The design strength profile used to predict the stability of the SDC under ice loading was based on the CPT data from the April 2005 investigation from the ice surface which was limited to depths of 12 m. The deeper CPT obtained in September 2005 from the deck of the SDC confirmed that the design profile was conservative. The design strength profile is shown by the solid black line on Figure 5.

Consolidated-undrained triaxial tests were done on three tube samples from the April 2005 investigation. Two tests were multistage to obtain effective stress strength parameters, and one test was single stage to observe the soil behaviour at large strains. The results of the consolidated-undrained triaxial tests on the samples from the April 2005 investigation are summarized in Table 1.

Table 1. Consolidated-undrained triaxial test results

Borehole	Depth (m)	σ'vo (kPa)	σ'c (kPa)	Su (kPa)	ϕ'	c'	Af	εi (%)	Ei (MPa)	εf (%)	Ef (MPa)
CPT05-01b	3.6	30	30	16	29°	0	0.55	0.1	7.1	3.3%	0.9
		30	80	36			0.58	0.2	15.5	3.7%	1.9
		30	130	71			0.44	0.3	17.9	7.8%	1.8
CPT05-02	1.1	9	60	38	n/a	n/a	0.45	0.1	12.5	9.6%	0.8
CPT05-03	1.2	10	10	16	26°	8	0.17	0.1	6.3	3.2%	1.0
		10	60	34			0.43	0.3	8.6	3.0%	2.2
		10	110	66			0.35	0.3	14.9	7.1%	1.9

Notes:
σ'_{v0} = insitu vertical effective stress
σ'_c = triaxial test consolidation pressure
S_u = undrained shear strength
ϕ'= effective stress strength parameters calculated from multistage tests only
A_f = pore pressure ratio calculated at failure or maximum test strain
ε_i and ε_f = strains for calculation of initial and final (maximum test strain) secant moduli
E_i and E_f = initial and final (maximum test strain) secant elastic moduli

3 DESIGN LOADING

Environmental loads considered for the SDC design included ice push, waves and earthquakes. The ice loading was the dominant loading case. B. Wright et al. (2005) assessed the ice loading conditions and the global ice load magnitudes at the Paktoa site for the SDC deployment. The recommended global design ice loads are summarized as follows:

•a maximum total design horizontal ice load against the long side of the SDC of 280 MN for the time period until late April; and

•a maximum total horizontal ice load of 420 MN for large multi-year ice floes up to 5 m thick against the long side of the SDC.

Vertical ice loads result from the weight of ice over the horizontal and sloping faces of the MAT. Two vertical ice loading scenarios were assumed for each horizontal load condition considered for calculations of the SDC stability: a vertical ice load magnitude equivalent to 10% and 130% of the horizontal ice load. These values are considered to encompass the range of likely values (B. Wright et al 2005). The vertical ice load was assumed to act at the mid-point of the sloping face of the MAT, approximately 15 m from the outer edge of the MAT.

4 DESIGN STABILITY AND DEFORMATION ANALYSES

The factor of safety against sliding under ice loading was calculated using limit equilibrium methods (Slope/W software), finite difference progressive strength reduction methods (FLAC software) and by hand calculation. The analyses were two-dimensional and assumed loading along the long face of the SDC and MAT. Three-dimensional effects such as the resistance of the soil along the sides of the shear surface surrounding the MAT are expected to increase the actual factor of safety by approximately 5%. The calculated factor of safety by each of these methods is shown as a function of horizontal ice load on Figure 6. Two vertical load cases are shown, where the assumed vertical ice load on the MAT is either 10% or 130% of the horizontal load.

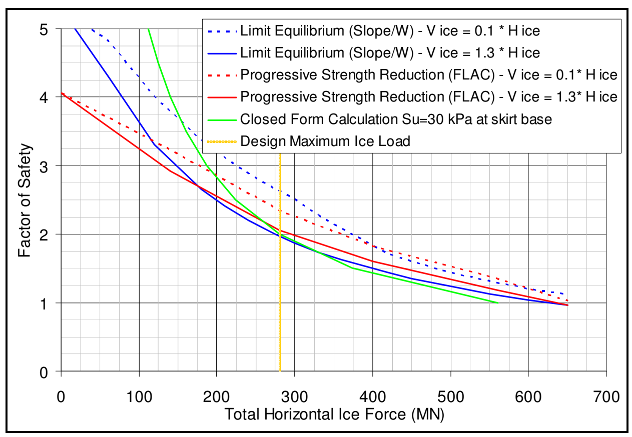

Figure 6. Calculated factor of safety based on horizontal ice load

The deformation response under load was predicted using the hyperbolic model formulated by Duncan and Chang (1970), with the Sigma/W finite element software. The parameters used for the analysis are listed in Table 2. With the exception of the Poisson's ratio and the unload-reload modulus number, these parameters were all obtained from the triaxial testing. Poisson's ratio was assumed to equal 0.45 for the saturated clay with limited drainage. The unload-reload modulus number was assumed to be approximately twice the initial loading modulus number, however, no test data were available to substantiate this assumption.

These parameters gave a good match with the stress-strain curves in the triaxial tests except for the tests at the very lowest confining stresses.

Table 2 – Hyperbolic model parameters

Parameter	Value	Description
Rf	0.9	Ratio of ultimate to failure deviatoric stress
ϕ	20°	Total stress friction angle
c	3 kPa	Total stress cohesion
K_i	169	Initial modulus number
K_{ur}	300	Unload-reload modulus number
n	0.64	Modulus exponent
ν	0.45	Poisson's ratio

The predicted load-deformation response is shown on Figure 7. This plot shows the deformation that would be measured over the depth range of the in-place inclinometers. Some further deformation below this depth was predicted by the numerical models, however, the installed instrumentation provided no means of measuring the actual deformation at greater depths, so the predicted deformation predictions are shown only over the measureable interval. Predicted deformation curves are shown for a location near the loaded edge of the SDC and under the centre of the SDC.

The irrecoverable deformation was estimated using the finite element model by including an unload/reload modulus stiffer than the initial loading modulus. For a horizontal ice load of 140 MN, the irrecoverable deformation was estimated to be approximately 30% of the total deformation during loading.

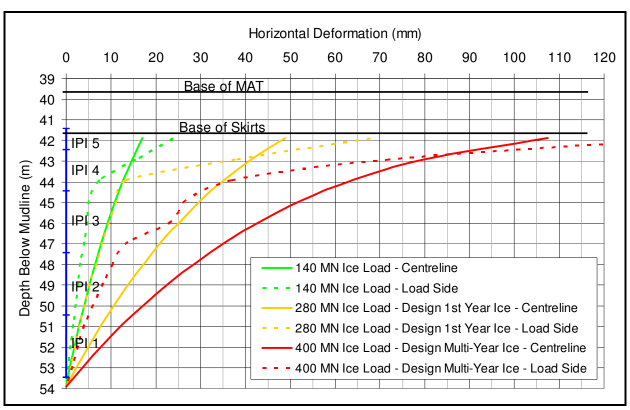

Figure 7. Predicted total horizontal deformation due to lateral ice loading

5 INSTRUMENTATION

The instrumentation installed in the seabed included two push-in piezometers in Tubes #7 and #9 for measuring the pore-water pressure in the SDC foundation, and an inclinometer casing in Tube #3 to allow the vertical profile of horizontal deformation to be measured. The locations of the instruments are shown in plan and section on Figures 4 and 8.

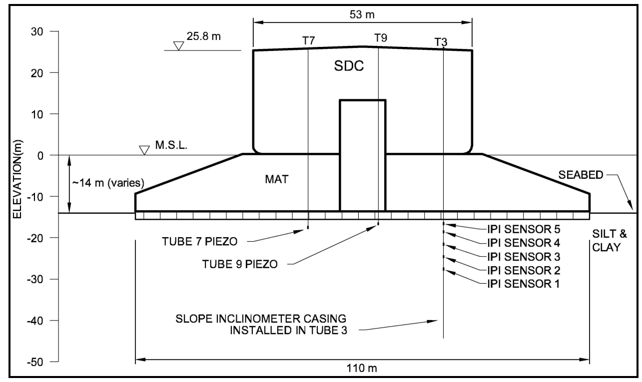

Figure 8. SDC cross-section with instrument locations

A string of 5 In-Place Inclinometers (IPIs) was installed in the inclinometer casing in December 2005 to monitor deformations in the zone below mudline. These sensors had individual lengths ranging from 1 m to 3 m. The entire sensor string monitored the range from 41.45 m below deck to 53.45 m below deck. This range of sensor coverage was set to encompass the majority of displacement anticipated in the foundation. A schematic diagram of the IPI installation is shown in Figure 9.

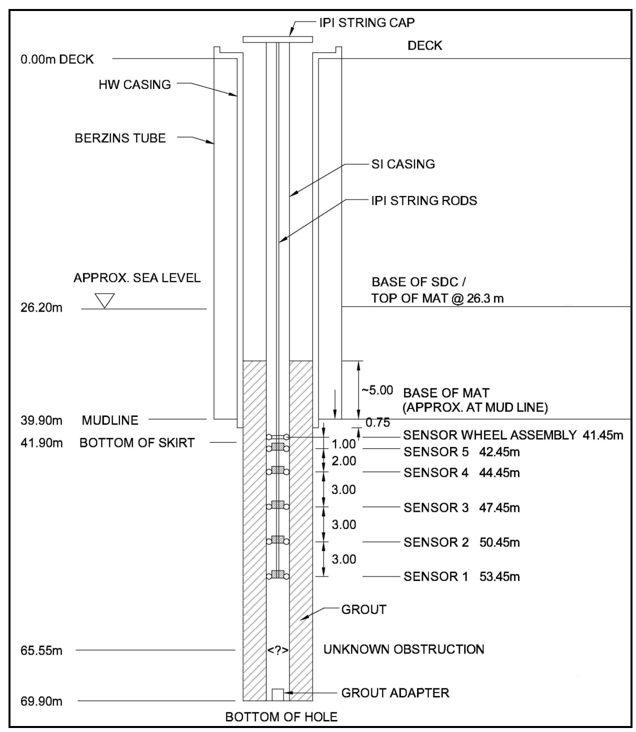

Figure 9. In-place inclinometer installation schematic

Prior to installing the IPIs, the inclinometer casing was surveyed using two manual inclinometer probes. The inclinometer casing was also surveyed with a spiral probe to identify the extent of twisting of the casing that had occurred during installation. This survey indicated that casing twist was limited to 5 degrees.

Following completion of the CPT, the holes in Tubes #7 and #9 were grouted to mudline, and a push-in electrical piezometer was installed below the skirt depth in each of these two holes.

The IPIs and piezometers were connected to dataloggers. Data from the IPIs and piezometers were once per minute and hourly, respectively. Manual readings of the inclinometer casing were taken prior to installation of the IPIs and following removal of the IPI sensors in August 2006.

The individual IPI sensors were subject to electrical noise with a peak to peak amplitude equivalent to approximately 2 mm deflection per metre of sensor length. This noise is evident in the IPI data plotted on Figure 10, however, the interpretation of the overall trends were not affected by this data noise.

6 SDC PAKTOA DEPLOYMENT

6.1 Setdown

The MAT has a flat bottom, with a network of skirts that extend 2 m below the base of the MAT to form a grid. The skirts penetrate into the seabed during setdown, to increase the lateral resistance to sliding of the SDC. Depending on the strength of the shallow seabed, the skirts may or may not penetrate the full 2 m into the seabed. During setdown at Paktoa, the skirts penetrated close to the full 2 m so that the base of the MAT was generally in contact with the seabed. Due to variations in the seabed topography, however, it is likely that gaps existed between the seabed and the base of the MAT in some areas. Initial setdown of the SDC at Paktoa C-60 was on August 27, 2005, with the bow oriented to the north-west. Maximum penetration of the skirts was achieved at 16.5 kPa contact pressure. The ballast was increased to temporarily preload the foundation to 59 kPa for about one day, and then the ballast was reduced to a final contact pressure of 49.5 kPa on September 1, 2005.

6.2 February 2006 Ice Event

Little significant movement occurred in the first two months following the installation of the IPI sensors. By mid February 2006, the net cumulative displacement was approximately 6 mm in the aft direction and zero in the port/starboard direction.

The greatest single ice loading event experienced over the 2005-2006 SDC deployment occurred over approximately 24 hours from the evening of February 21 to the evening of February 22, 2006. At this time, the ice surrounding the SDC was landfast and approximately 1 m thick. The total horizontal ice movement was in the range of 1.0 to 1.15 m with sustained wind speeds of 80 km/h and higher gusts (Sudom and Timco, 2008).

During this event, the SDC experienced horizontal displacement of approximately 24 mm in the starboard direction and 24 mm in the aft direction, or a vector displacement of 34 mm at 135° clockwise from the forward direction. The displacement vector was in agreement with the ice load direction, which was from the west, impacting the SDC from the forward port corner.

Some elastic rebound was experienced shortly after the initial displacement. This rebound caused a horizontal displacement of 6 mm in the port direction and 8 mm in the forward direction. The rebound occurred over 2 to 3 days following the ice loading event.

Accounting for the rebound, the net displacement from the ice loading event was 18 mm in the starboard direction and 16 mm in the aft direction for a vector displacement of 24 mm at 138° from the forward direction. The displacement measured at the in-place inclinometer location and the movement direction vectors are shown on Figure 10 and Figure 11.

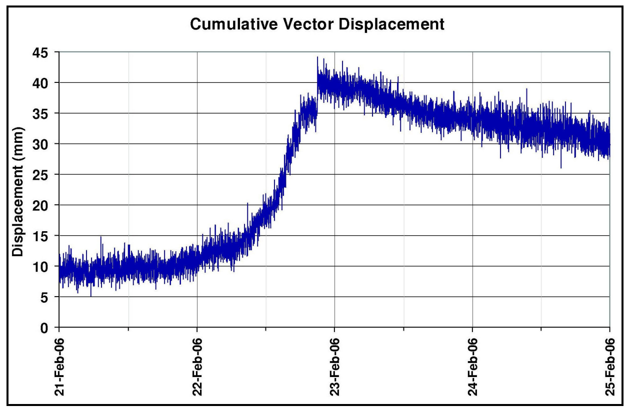

Figure 10. Measured displacement and displacement vector with instrument locations

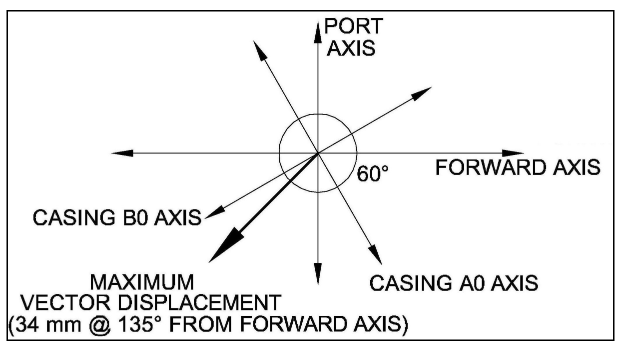

Figure 11. Inclinometer displacement vectors

The IPI and manual inclinometer readings show that the horizontal deformation occurred primarily in the upper 15 m of the seabed, with the greatest strains in the first 2 m below the base of the skirts. A plot of the manual inclinometer readings prior to and following the ice loading event are shown on Figure 12. The total displacement shown includes minor further displacements that occurred following the February 2006 ice loading event. A photo of the SDC taken in March 2006 showing ice rubble on the port side and rubble buildup on the forward port corner is shown on Figure 13.

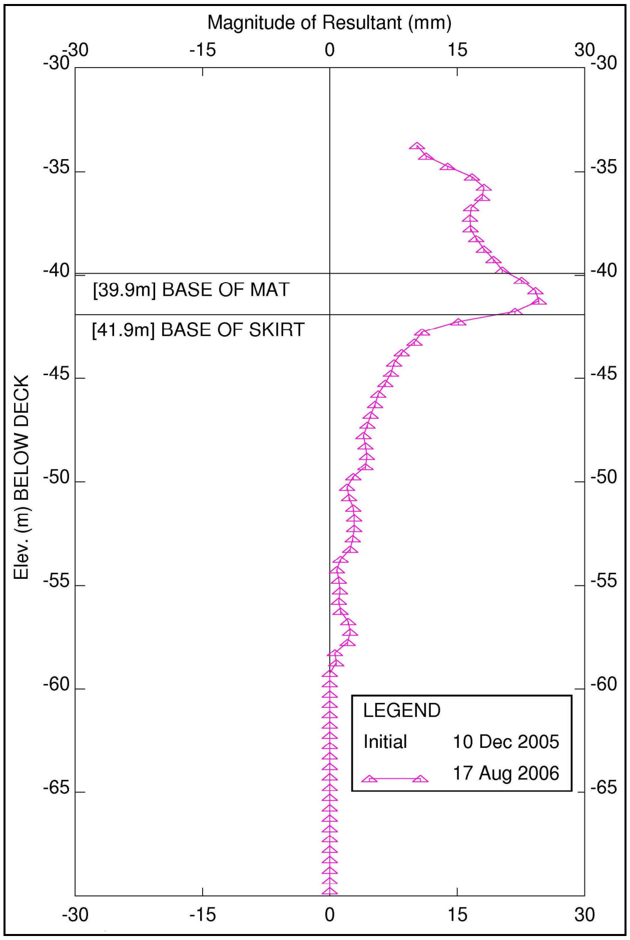

Figure 12. Manual inclinometer plot following ice loading

Figure 13. SDC with ice rubble – March 2006

7 POST-EVENT ANALYSES

Following the February 2006 ice loading event, ice loads on the SDC and foundation soils were modelled numerically to estimate the ice loads, based on matching the deflections recorded at the inclinometer location. The ice loads were separately estimated to be in the range of 55 to 89 MN based on consideration of buckling resistance of the ice and the local lateral resistance of the MAT skirts (Sudom and Timco, 2008).

Further load-deformation analyses of the foundation soils were also undertaken to estimate the total ice load. These analyses used both the 2D and 3D versions of the finite difference software FLAC. The soil strengths used in the numerical analyses were based on the CPT soundings, and the soil moduli were estimated based on the triaxial tests and correlations with the undrained shear strengths calculated from the CPT. The post-event analyses used best-estimate soil strengths as opposed to the more conservative design values. A simple Mohr-Coulomb model was used for these post-event analyses. The soil moduli were assumed to increase with depth and ranged from 3 MPa near the ground surface to 17 MPa below 20 m depth.

The deformations due to ice loading predicted using the 3D FLAC analyses within the inclinometer measurement depth range are shown on Figure 14. The predicted foundation displacements at the base of the skirts for a 120 MN global ice load are shown on Figure 15, normalized to zero displacement at the base of the inclinometer casing.

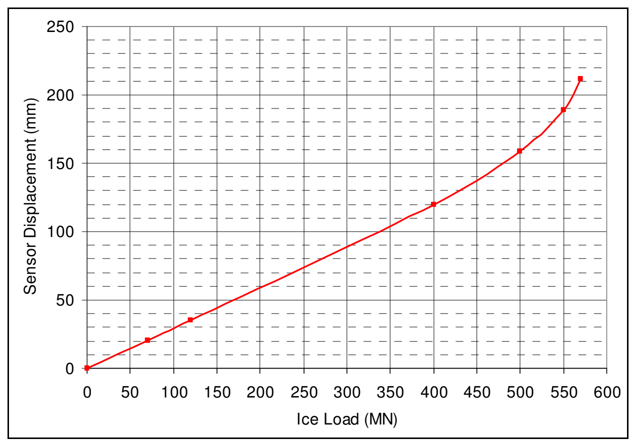

Figure 14. Predicted soil displacement versus ice load within inclinometer depth range

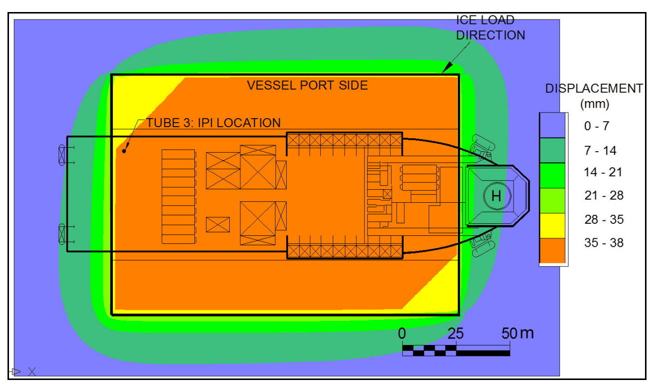

Figure 15. Foundation displacements at 120 MN load

The total deformation recorded by the inclinometer during the February 2006 ice event was 34 mm, with

10 mm of rebound following removal of the ice load. The numerical models did not predict significant soil yielding for the ice load magnitude, and lower plastic (permanent) deformations than were recorded by the inclinometers. Part of the observed permanent deformation may be a result of the inclinometer casing being dragged slightly through the soft soil by the movement of the SDC. A steel “foot” was present on the base of each of the skirts which was wider than the skirt. As a result a vertical gap may have existed between the web of each skirt and the soil following setdown, or, if the soil flowed back against the skirts, this soil would be highly disturbed. The SDC would therefore have to move horizontally prior to mobilizing the passive resistance of the soil against the skirts, and transferring the shear stress to the foundation under the SDC. This initial movement would be largely un-recoverable, and may have caused the inclinometer casing to drag deeper into the soft foundation soils. As a result, the most reliable estimate of the horizontal ice load is likely somewhere between the magnitude calculated based on the total displacement, and the magnitude calculated considering only the elastic portion of the displacement.

The finite difference mesh used in these analyses didn’t model the details of the skirts and the local interaction between the skirts and the foundation soils above the skirt base. The SDC was modelled as a rigid body, and so possible compliance of the SDC and MAT under ice loading was not considered.

From Figure 14, the ice loads corresponding to the 34 mm (total) and 10 mm (elastic) deformation are 110 MN and 30 MN respectively. The actual ice load was probably somewhere in this range. A more definitive load estimate is not possible from the soil and deformation data available. The global load estimates based on the soil deformations encompasses the range of estimates reported by Sudom and Timco (2008).

The Mohr-Coulomb model is recognized to have a number of limitations, including poor handling of deformations as portions of the domain start to yield. The limited laboratory test data available for the foundation clays did not warrant consideration of a more sophisticated constitutive model, however. The results are likely reasonable for the relatively low loads encountered by the SDC. Accurate modelling of the deformation patterns as the ice loads approach the ultimate strength would require a more extensive foundation investigation program, additional lab testing and greater modelling sophistication.

8 RECOMMENDATIONS FOR FUTURE DEPLOYMENTS

Model calibration was difficult with the single inclinometer. Further deployments should have a minimum of two and preferably four in-place inclinometer strings to measure real-time deformation of the seabed. The greater number of inclinometers will also allow measurement of rotation of the structure that may occur due to asymmetrical ice loading.

Precise GPS measurements at different locations on the SDC could also be used to estimate the rotation of the SDC, even if the GPS measurements at this remote location were insufficiently accurate to track the absolute displacement vector.

ACKNOWLEDGEMENTS

The authors acknowledge and appreciate the permission of Devon Canada Corporation to publish the data contained in this paper, and in particular the support of Bill Livingstone and Peter Millman. The insights of Kevin Hewitt into the SDC-foundation interaction were helpful in understanding the system performance.

REFERENCES

B. Wright and Associates, K.R. Croasdale and Associates, and Sandwell Engineering. 2005. *Global Ice Load Design Criteria for the SDC at Devon Canada’s Paktoa B-60 Drilling Site.* Report submitted to Devon Canada, March.

Blasco, S.M., Fortin, G., Hill, P.R., O’Connor, J.J. and Brigham-Grette, J., 1990. The Late Neogene and Quaternary Stratigraphy of the Canadian Beaufort Continental Shelf. The Arctic Ocean Region: Boulder, Colorado, Geological Society of America, *The Geology of North America*, vol. I, Chapter. 26, pp. 491-502.

Duncan, J., and Chang, C-Y. 1970. Nonlinear Analysis of Stress and Strain in Soils. *Journal of the Soil Mechanics and Foundation Division*, ASCE, 96(SM5): 1629-1653.

Hewitt K.J., Sladen J.A., Williams D.R., and Brown J. 1987. Geotechnical Evaluation and Performance of the Canmar SSDC/MAT Mobile Offshore Drilling Unit. *Canadian Geotechnical Conference*. 364-372.

Jefferies, M., Ruffell, J., Crooks, J., and Hughes, J. 1985. Some Aspects of the Behavior of Beaufort Sea Clays. *Strength Testing of Marine Sediments, Laboratory and In-Situ Measurements*, ASTM STP 883, Chaney and Demars, Eds. 487-514.

O’Connor, M.J., 1980. *Development of a Proposed Model to Account for the Surficial Geology of the Southern Beaufort Sea*. A report for the GSC, Contract No. OSC70-00212, GSC open file report No. 954.

O’Connor, M.J., 1982. *An Evaluation of the Regional Surficial Geology of the Southern Beaufort Sea*. Report prepared for GSC, Contract No. 07SC-23420-1-M562.

Shinde, S., Crooks, J., James, D., and Fitzpatrick, S.W. 1986. Geotechnical Design for Beaufort Sea Structures. *3rd Canadian Conference on Marine Geotechnical Engineering*, St. John’s., 347-362.

Sudom, D., and Timco, G. 2008. Analysis of Loads on the SDC at Paktoa C-60 during an Ice Creep Buckling Event. *19th IAHR Symposium on Ice*. Vol 2: 897-907.

Weaver, J. and Poplin, J. 1997. A case history of the Nipterk P-32 spray ice island. *Canadian Geotechnical Journal,* 34:1-16.